

ANL-6247  
Physics and Mathematics  
(TID-4500, 15th Ed.)  
AEC Research and  
Development Report

ARGONNE NATIONAL LABORATORY  
9700 South Cass Avenue  
Argonne, Illinois

THE FISSION ENERGETICS OF Th<sup>232</sup>

by

A. B. Smith  
R. G. Nobles

Reactor Engineering Division

and

A. M. Friedman

Chemistry Division

November 1960

Operated by The University of Chicago  
under  
Contract W-31-109-eng-38

## **DISCLAIMER**

**This report was prepared as an account of work sponsored by an agency of the United States Government. Neither the United States Government nor any agency Thereof, nor any of their employees, makes any warranty, express or implied, or assumes any legal liability or responsibility for the accuracy, completeness, or usefulness of any information, apparatus, product, or process disclosed, or represents that its use would not infringe privately owned rights. Reference herein to any specific commercial product, process, or service by trade name, trademark, manufacturer, or otherwise does not necessarily constitute or imply its endorsement, recommendation, or favoring by the United States Government or any agency thereof. The views and opinions of authors expressed herein do not necessarily state or reflect those of the United States Government or any agency thereof.**

## **DISCLAIMER**

**Portions of this document may be illegible in electronic image products. Images are produced from the best available original document.**

## TABLE OF CONTENTS

	<u>Page</u>
ABSTRACT . . . . .	4
I. INTRODUCTION. . . . .	4
II. EXPERIMENTAL PROCEDURE . . . . .	5
III. RESULTS . . . . .	6
IV. CONCLUSIONS. . . . .	7
V. ACKNOWLEDGMENTS . . . . .	9
REFERENCES . . . . .	9

## LIST OF TABLES

<u>No.</u>	<u>Title</u>	<u>Page</u>
1.	Thorium-232 Fission Properties. . . . .	7

## LIST OF FIGURES

<u>No.</u>	<u>Title</u>	<u>Page</u>
1.	Block Diagram of Electronic Circuitry. . . . .	11
2.	Topological Plot of Th <sup>232</sup> Fission Fragment Distribution for Incident Neutron Energies of 1.475 and 1.600 Mev . . . . .	12
3.	Th <sup>232</sup> Fission Fragment Energy Distribution Observed on One Side of Back-to-Back Ionization Chamber . . . . .	13
4.	Distribution of Total Kinetic Energy of Fragments from 1.475 Mev and 1.600 Mev Neutron-Induced Fission of Th <sup>232</sup> . . . . .	14
5.	Distribution of Fragment Mass Ratio for 1.475 Mev and 1.600 Mev Neutron-Induced Fission of Th <sup>232</sup> . . . . .	15
6.	Primary Mass Yield from Fission of Th <sup>232</sup> , Chemical Data Points from Katcoff <sup>(19)</sup> and Shown for Comparison. . . . .	16
7.	Average Total Kinetic Energy as a Function of Mass Ratio for Fragments from 1.475 Mev and 1.600 Mev Neutron-Induced Fission of Th <sup>232</sup> . . . . .	17
8.	Total Fragment Kinetic Energies and Primary Mass Yields of Known Spontaneous and Slow Neutron ( $E_n = \leq 1.5$ Mev) Induced Fission Process . . . . .	18
9.	Anisotropy of Th <sup>232</sup> Fission Measured by Henkel and Brolley <sup>(10)</sup> . . . . .	19
10.	Measured Angular Distribution of Th <sup>232</sup> Fragment Anisotropy. Theoretical Components of the Distribution (Inset) are from Willets and Chase <sup>(7)</sup> . . . . .	20

THE FISSION ENERGETICS OF Th<sup>232</sup>

by

A. B. Smith, A. M. Friedman, and R. G. Nobles

## ABSTRACT

The distribution of the kinetic energy of fragments emitted as a result of the neutron-induced fission of thorium-232 has been determined. Incident neutron energies of  $1475 \pm 35$  kev and  $1600 \pm 35$  kev were used. The distributions determined at the two incident neutron energies are identical. The measured total average fragment kinetic energy was  $155 \pm 4.5$  Mev. The most probable fragment mass ratio is  $1.47 \pm 0.05$ , and the average kinetic energies of the light and heavy fragments are  $95 \pm 2$  and  $60 \pm 3$  Mev, respectively. The experimental results have been related to the known systematics of neutron-induced and spontaneous fission. The effect of collective nuclear rotations at the saddle point is discussed, with particular emphasis on fission from specific rotational bands.

## I. INTRODUCTION

The large kinetic energy of the massive fission fragments emitted at neutron-induced fission is the basis for many applications of nuclear energy. Thus it is not strange that, since the discovery of fission, a large number of studies of fragment kinetic energies have been undertaken. Some of the early work dealt with the neutron-induced fission of thorium-232.<sup>(1,2)</sup> The results of these investigations are amazingly accurate in view of the techniques contemporary to the period. However, this early work did not give a detailed knowledge of the thorium-232 fission process and the results are in some disagreement with currently accepted systematics of fission.<sup>(3)</sup> Recently, fragment studies of thorium-232 fission induced by 14.9-Mev neutrons have given a clear picture of the process at this relatively high incident neutron energy.<sup>(4)</sup>

Soon after the discovery of fission, the single-particle aspects of the nucleus were related to the characteristic fission mass asymmetry.<sup>(5)</sup> Recently, the theory of collective nuclear motions has been utilized to interpret the nuclear structure of heavy elements and has been extended to studies of the fission process.<sup>(6-9)</sup> The collective interpretation of fission has been remarkably successful in explaining the gross and detailed features of the angular correlation between the incident particle and the

fission fragment axis.<sup>(8,9)</sup> The unique dependence of the thorium-232 fission fragment angular anisotropy on the incident neutron energy has been very nicely interpreted in terms of the collective model.<sup>(7,10)</sup> Thorium-232 fission anisotropy displays a very sharp shift toward  $90^\circ$  at incident neutron energies corresponding to the first "giant resonance" just above threshold ( $E_n = 1.6$  Mev).<sup>(11)</sup> This abrupt change in anisotropy is attributed to fissile nuclei crossing the saddle point in energy states belonging to the  $K = 3/2$  rotational band. At incident energies above or below 1.6 Mev, rotational bands characterized by  $K \neq 3/2$  are predominant at the saddle point and lead to less energy-dependent and smaller anisotropy. Thus a detailed comparison of the properties of thorium-232 fission induced by neutrons of 1.6 Mev with that induced by neutrons of sufficiently different energy to provide large contributions from rotational bands other than  $K = 3/2$  should indicate how deeply the rotational structure at the saddle point effects the fission process.

In view of the theoretical aspects of thorium-232 fission outlined above and because of the growing importance of thorium-232 in many nuclear applications, this experimental study of the neutron induced fission of thorium-232 was undertaken.

## II. EXPERIMENTAL PROCEDURE

A  $50\text{-}\mu\text{gm}/\text{cm}^2$  sample of thorium-232 was electrochemically deposited onto a  $25\text{-}\mu\text{gm}/\text{cm}^2$  Zapon film. This source was supported over a 5-inch diameter area by a Lektromesh grid.<sup>(12)</sup> The completed sample was placed between two halves of a conventional back-to-back electron collection chamber.<sup>(13)</sup> The chamber was carefully evacuated before each run and then filled to an atmosphere and a half with a mixture of 90% argon and 10% methane. Under these conditions the resolution of the detector for 5-Mev alpha particles was 1 to 2%, full width at one-half maximum.

The voltage pulses derived from the electron collection chamber were amplified and converted to digital information. This digital representation of the ionization occurring within the chamber was recorded in such a manner that the one-to-one time correlation between the two fragments resulting from a given fission event was maintained. Final data reduction was carried out with the aid of a digital computer. The actual electronic circuitry utilized is shown schematically in Fig. 1.

The analyzed proton beam from a Van de Graaff accelerator was used to produce neutrons by means of the  $\text{Li}^7(p,n)\text{Be}^7$  reaction.<sup>(14)</sup> The fission chamber was placed near the target. The geometry and target thickness were arranged so as to provide a neutron energy spread of  $\lesssim 70$  kev at the thorium sample. The mean energy of the incident neutrons was known to  $\pm 5$  kev. The chamber was frequently rotated to avoid any possible angular-dependent effects due to the chamber structure or source support.

The experiment was executed on three separate occasions spread over some eighteen months. Each experiment consisted of four separate measurements, two at an average incident neutron energy of 1600 kev and two at 1475 kev. Following the measurements, a comparison of the thorium-232 fragment energies with those resulting from californium-252 spontaneous fission was made.<sup>(15,16)</sup> The californium secondary standard was calibrated against uranium-235 thermal neutron-induced fission.<sup>(17)</sup> Since thorium-232 and uranium-235 fission fragment energies are not widely different, this method of energy calibration avoids any significant errors due to the energy and mass dependence of the ionization defect.<sup>(18)</sup>

### III. RESULTS

The prominent characteristics of thorium fission are shown in Fig. 2. It is at once evident that there is no pronounced difference between thorium fission induced by 1.475-Mev neutrons and that induced by 1.600-Mev neutrons. Actually, any differences between the two plots in Fig. 2 are well within the statistical uncertainty of the measurements. A typical "one-sided" fragment energy distribution is shown in Fig. 3. This two-dimensional distribution can be obtained from Fig. 2 by reflection of the latter about the line of symmetry and projection to either of the individual fragment energy axes. The apparent peak to valley ratio in Fig. 3 is 12:1, indicating a large fission asymmetry and good chamber resolution.

Summing, in a one-to-one manner, the two fragment energies resulting from the binary thorium fission yields the total fragment kinetic energy distribution shown in Fig. 4. The average total fragment kinetic energies at the two incident neutron energies are essentially equivalent. The full widths at half maximum of the distributions agree within the experimental error of  $\sim \pm 1.0\%$ . Similar total energy distributions were obtained at specific mass ratios. Although of less precision, these results clearly indicate that the speed in total fragment kinetic energy is smallest at the most probable mass split.

Figures 5 and 6 show, respectively, the mass ratio distribution and mass yield as determined in this experiment. In Fig. 6 the primary mass yield curve obtained from chemical studies is compared with this work, assuming<sup>(19)</sup> a value of  $\bar{\nu} = 3.0$ . The agreement with the chemical data is reasonable in view of the uncertainties of the chemical measurements and the fact that the two techniques really measure different quantities. The chemical values must be extrapolated over a three-dimensional charge-mass surface to the primary yields while the detector in this experiment actually measures ionization, a quantity slightly dependent on the mass and charge of the massive particles. Another source of possible variation between the chemical and ionization mass yield curves is the energy of incident neutrons. In the chemical studies fission was induced by "fast" neutrons while this experiment utilized neutrons of specific energies.



The dependence of the total fragment kinetic energy on mass ratio is shown in Fig. 7. The qualitative shape of the curves is characteristic of asymmetric fission. However, there is a rather more pronounced decrease in the total energy as symmetry is approached than is evidenced in most fission. (15,17,20)

The characteristics of thorium fission illustrated in the above figures are numerically summarized in Table I. The table also gives results from other pertinent work. From the table it is evident that the fragment kinetics of thorium-232 fission induced by 1.475, 1.600 and 14.0 Mev-neutrons are similar. However, a detailed comparison of this work with that of Protopopov *et al.* (4) shows that the probability of symmetric fission increases by at least an order of magnitude when the incident neutron energy is raised from 1.600 to 14.9 Mev.

Table I

THORIUM-232 FISSION PROPERTIES

Average Incident Neutron Energy (Mev)	Average Kinetic Energy, Light Fragment (Mev)	Average Kinetic Energy, Heavy Fragment (Mev)	Total Average Fragment Kinetic Energy (Mev)	Most Probable Mass Ratio	Reference
1.475	95 ± 2	60 ± 3	155 ± 4.5	1.47 ± 0.05	This work
1.600	95 ± 2	60 ± 3	155 ± 4.5	1.47 ± 0.05	This work
14.9	96*	62*	157 ± 4.0*	1.43 ± 0.05	4
"fast"	91*a	60*a		1.51†a	1
"fast"	92.6*a	58.3*a		1.59†a	2

a. Not corrected for ionization defect.

† "Single sided" measurements giving peak ratios only.

\* Denotes most probable values.

#### IV. CONCLUSIONS

From the above experimental results it is evident that thorium-232 fission induced by 1.600-Mev neutrons is experimentally indistinguishable from that produced by 1.475-Mev neutrons. The process is a highly asymmetric neutron-induced fission qualitatively similar to the slow neutron fission of uranium-235. The mass asymmetry and total kinetic energy of the fragments agree very well with the systematics of neutron induced and spontaneous fission. (16,3) This is illustrated in Fig. 8. The thorium-232 total kinetic energy continues the trend toward decreasing energy with smaller values of the parameter  $Z^2/A^{1/3}$ . (21,16) The mass of the thorium-232 heavy fragment is 138, in agreement with the systematic constancy of this quantity for all fissile nuclei that have neutron numbers less than 152.

The anisotropy of thorium-232 fission fragments near threshold, as measured by Henkel and Brolley,<sup>(10)</sup> is shown in Fig. 9. Clearly evident is the pronounced dip in  $\omega(0^\circ)/\omega(90^\circ)$  (fragment emission in the direction of incident neutrons/perpendicular fragment emission) corresponding to the sharp peak in the fission cross section. Using the Bohr collective model,<sup>(6,8)</sup> Willets and Chase<sup>(7)</sup> have explained the thorium angular anisotropy at an incident neutron energy of 1.600 Mev. Their fit to the experimental distribution of Henkel and Brolley<sup>(10)</sup> is shown in Fig. 10. From this figure it is evident that the angular distribution of the anisotropy tends to zero at zero degrees in a very precipitous manner. Such behavior in terms of the collective model can only be obtained by fission through saddle point states belonging to the  $K = 3/2$  rotational band. All other reasonable  $K$  bands result in angular distributions tending toward zero degrees with zero slope. The inset in Fig. 10 shows the contributions of the  $I = 3/2, 5/2$  and  $7/2$  total angular momentum components to the  $K = 3/2$  band necessary for the experimental fit. Analytically, this mixture is given by<sup>(7)</sup>

$$\omega(\theta) = 0.63 \omega_{3/2}^{3/2} + 0.18 \omega_{3/2}^{5/2} + 0.33 \omega_{3/2}^{7/2} + 0.68 \times 1/2$$

Thus it seems clear from the experimental and theoretical knowledge of anisotropy that a very large portion of thorium-232 fission at an incident neutron energy of 1.600 Mev proceeds through  $K = 3/2$  rotation saddle point states. All members of this band have the same parity.<sup>(7,8)</sup> Furthermore it is argued that  $\ell = 3$  neutrons are the major contributors to this band. Thus the parity of this set of levels must be negative. This assumption is supported by current optical model interpretations of neutron phenomena in this energy range.<sup>(22)</sup>

At a lower incident neutron energy of 1.475 Mev, the anisotropy of thorium fission is considerably smaller than that at  $E_n = 1.600$  Mev. This indicates that there are sizable fission contributions from saddle point rotational bands other than  $K = 3/2$ . As a result of the absence of any measurable differences in fission fragment energetics of mass asymmetries at the bombarding energies of 1.600 Mev and 1.475 Mev used in this experiment, we must conclude that fragment anisotropy and energetics are not sensitive to the rotational quantum number  $K$ .

In the above we have, a priori, assumed that the collective nuclear motion greatly influences fission at and just above threshold. It may well be that such basic phenomena as fission asymmetry are rooted very deeply in the energetics of fission. In this eventuality one would expect the collective nuclear motion to so slightly perturb the basic properties of the process as to make the measurement of the effect exceedingly difficult.

## V. ACKNOWLEDGMENTS

The authors are indebted to the Misses M. Schlapkohl and M. Miller for their aid in the processing of the data.

## REFERENCES

1. W. Jentschke, Energies and Masses of the Fission Fragments of Uranium Irradiated by Neutrons, *Zeits. f. Physik* 120, 165 (1943).
2. J. Fowler and L. Rosen, Energy Distribution of the Fragments Resulting from the Fission of  $U^{235}$  and  $Th^{232}$  by Slow and by Fast Neutrons, *Phys. Rev.* 72, 926 (1947).
3. I. Halpern, Nuclear Fission, a review in Annual Review of Nuclear Science, Vol. 9 (1959) Annual Reviews, Inc., Palo Alto, California.
4. Protopopov et al.,  $Th^{232}$  Fission Induced by 14.9-Mev Neutrons, *Zhurnal Eksperimentalnai I. Teoreticheskai Fiziki* 38, 384 (1960).
5. L. Meitner, Fission and Nuclear Shell Model, *Nature* 165, 561 (1950).
6. A. Bohr and B. Mottelson, Collective and Individual-Particle Aspects of Nuclear Structure, *Dan. Mat. Fys. Medd.* 27, No. 16 (1953).
7. L. Willets and D. Chase, Angular Distribution of Fission Fragments at Threshold According to the Bohr Model, *Phys. Rev.* 103, 1296 (1956)
8. A. Bohr, On the Theory of Nuclear Fission, Paper P/911, Vol. 2, Proceedings of the First International Conference on Peaceful Uses of Atomic Energy, United Nations Press, New York (1955).
9. J. J. Griffin, Energy Dependence of Fission Fragment Anisotropy, *Phys. Rev.* 116, 107 (1959).
10. R. L. Henkel and J. E. Brolley, Angular Distribution of Fragments from Neutron-induced Fission of  $U^{238}$  and  $Th^{232}$ , *Phys. Rev.* 103, 1292 (1956).
11. D. J. Hughes et al., Neutron Cross Sections, BNL-325 (July 1, 1958).
12. "Lektromesh," C. O. Jelliff Mfg. Corp., Southport, Connecticut.
13. O. Bunemann et al., Design of Grid Ionization Chambers, *Can. J. Res.* 27A, 191 (1949).

14. F. Ajzenberg and T. Lauritsen, Energy Levels of Light Nuclei. V, Rev. Mod. Phys. 27, 77 (1955).
15. J. C. D. Milton and J. L. Fraser, Fission Fragment Velocity Measurements and Coincident Gamma Spectra for Cf<sup>252</sup>, Chalk River Report PD-288.
16. A. B. Smith et al., An Experimental Study of Fission in the Actinide Elements, Paper P/690, Vol. 15, Proceedings of the Second International Conference on Peaceful Uses of Atomic Energy, United Nations Press, Geneva (1958).
17. W. Stein, Velocities of Fragment Pairs from U<sup>233</sup>, U<sup>235</sup>, and Pu<sup>239</sup> Fission, Phys. Rev. 108, 94 (1957).
18. R. Leachman, Velocities of Fragments from Fission of U<sup>233</sup>, U<sup>235</sup>, and Pu<sup>239</sup>, Phys. Rev. 87, 444 (1952).
19. S. Katcoff, Fission-Product Yields from U, Th and Pu, Nucleonics, Vol. 16 (No. 4), 78-85 (April 1958).
20. D. Brunton and G. Hanna, Energy Distribution of Fission Fragments from U<sup>235</sup> and U<sup>233</sup>, Can. J. Res. 28A, 190 (1950).
21. J. Terrell, Fission Neutron Spectra and Nuclear Temperatures, Phys. Rev. 113, 527 (1959).
22. P. Moldauer, private communication.

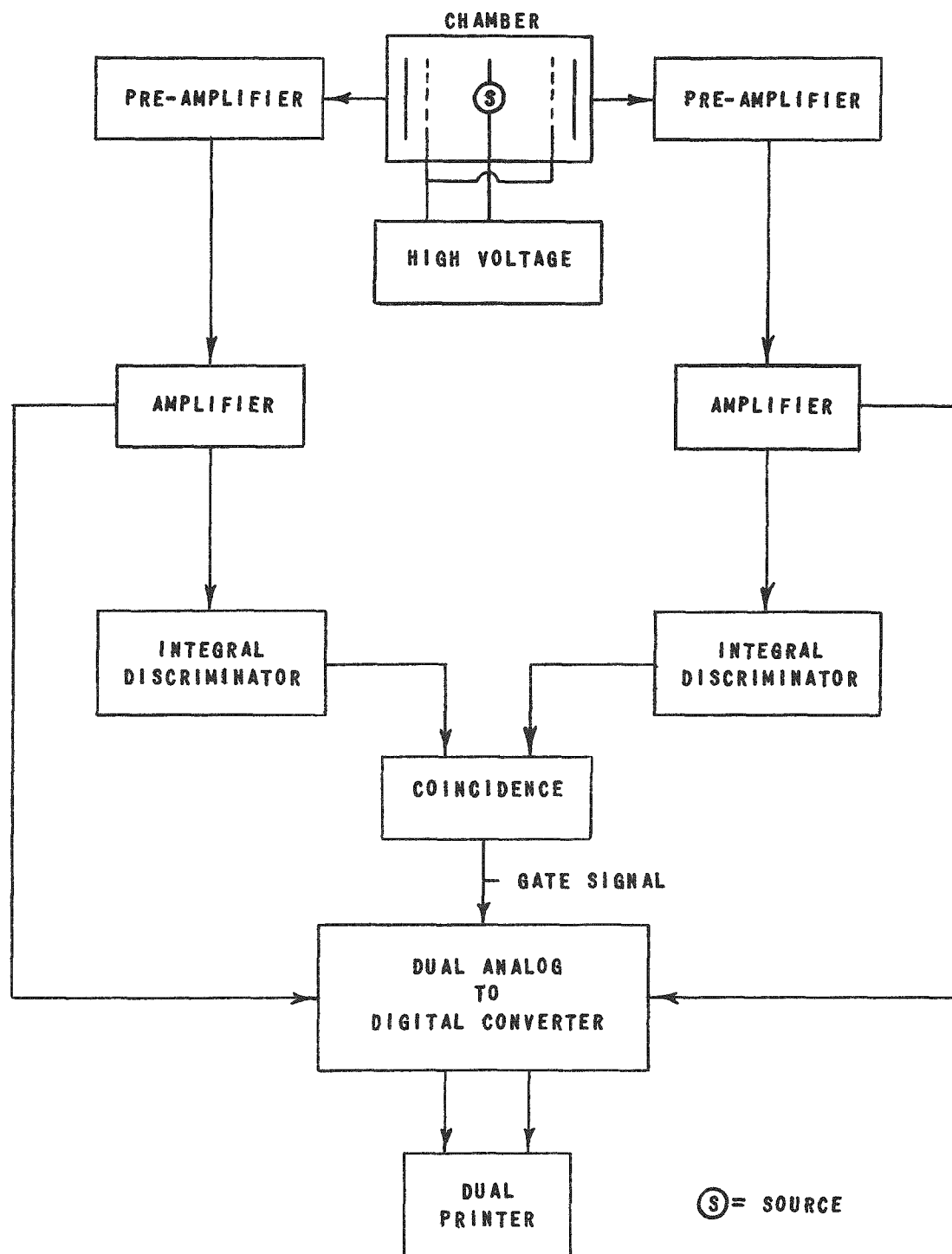


FIG. 1  
BLOCK DIAGRAM OF ELECTRONIC CIRCUITRY

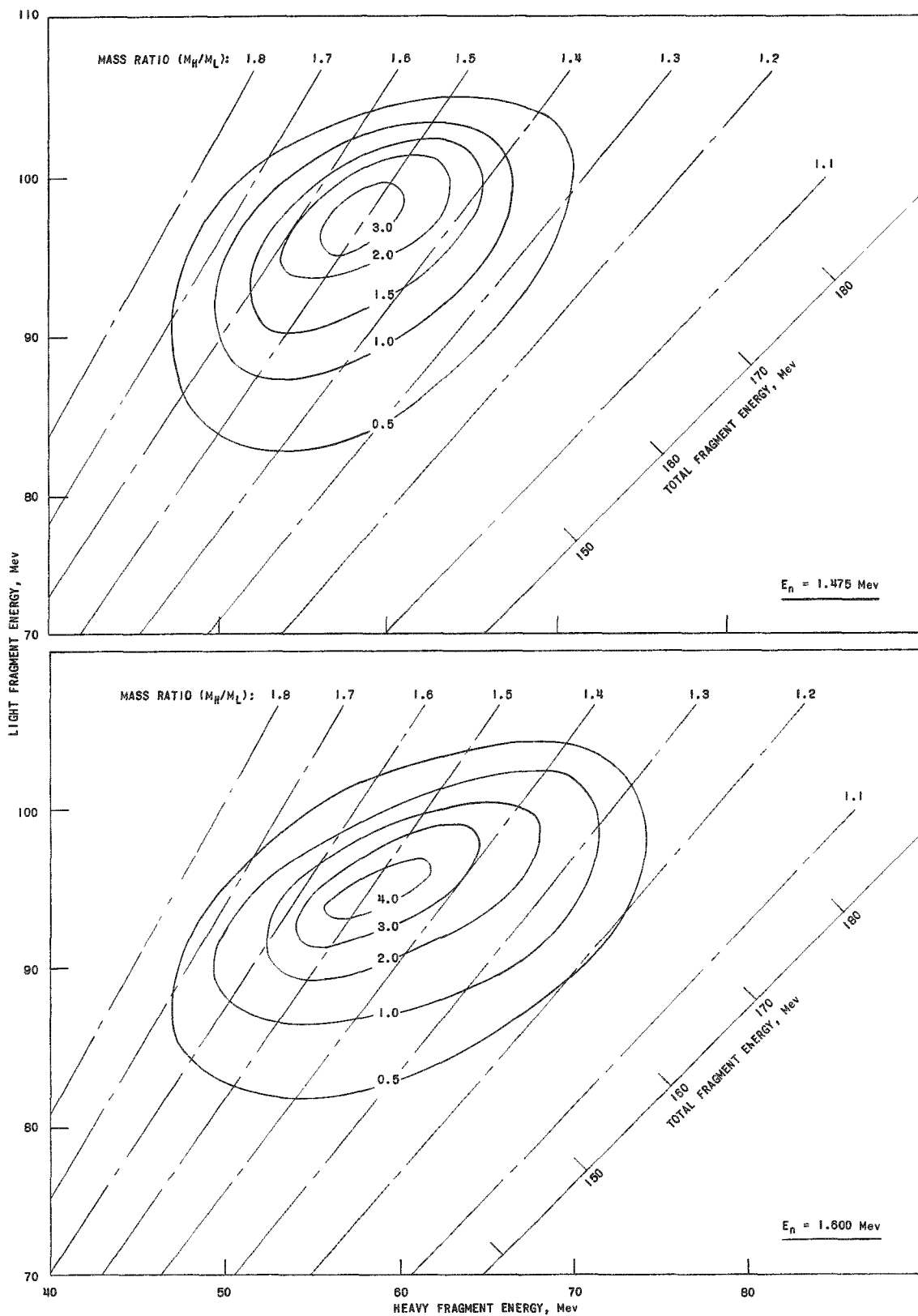


FIG. 2  
 TOPOLOGICAL PLOT OF  $\text{Th}^{232}$  FISSION FRAGMENT DISTRIBUTION FOR  
 INCIDENT NEUTRON ENERGIES OF 1.475 AND 1.600 Mev.

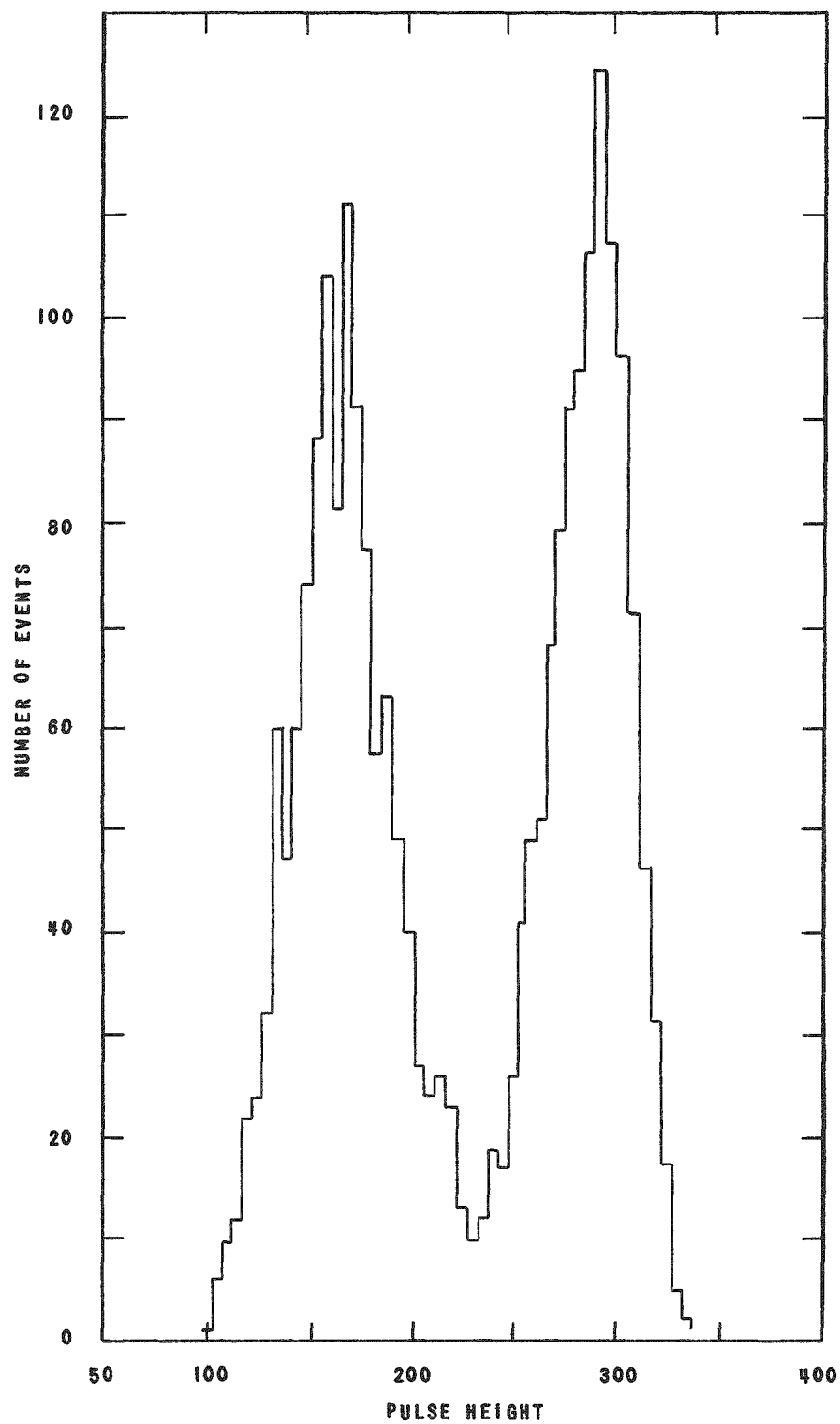


FIG. 3  
 $\text{Th}^{232}$  FISSION FRAGMENT ENERGY  
DISTRIBUTION OBSERVED ON ONE SIDE  
OF BACK-TO-BACK IONIZATION CHAMBER.

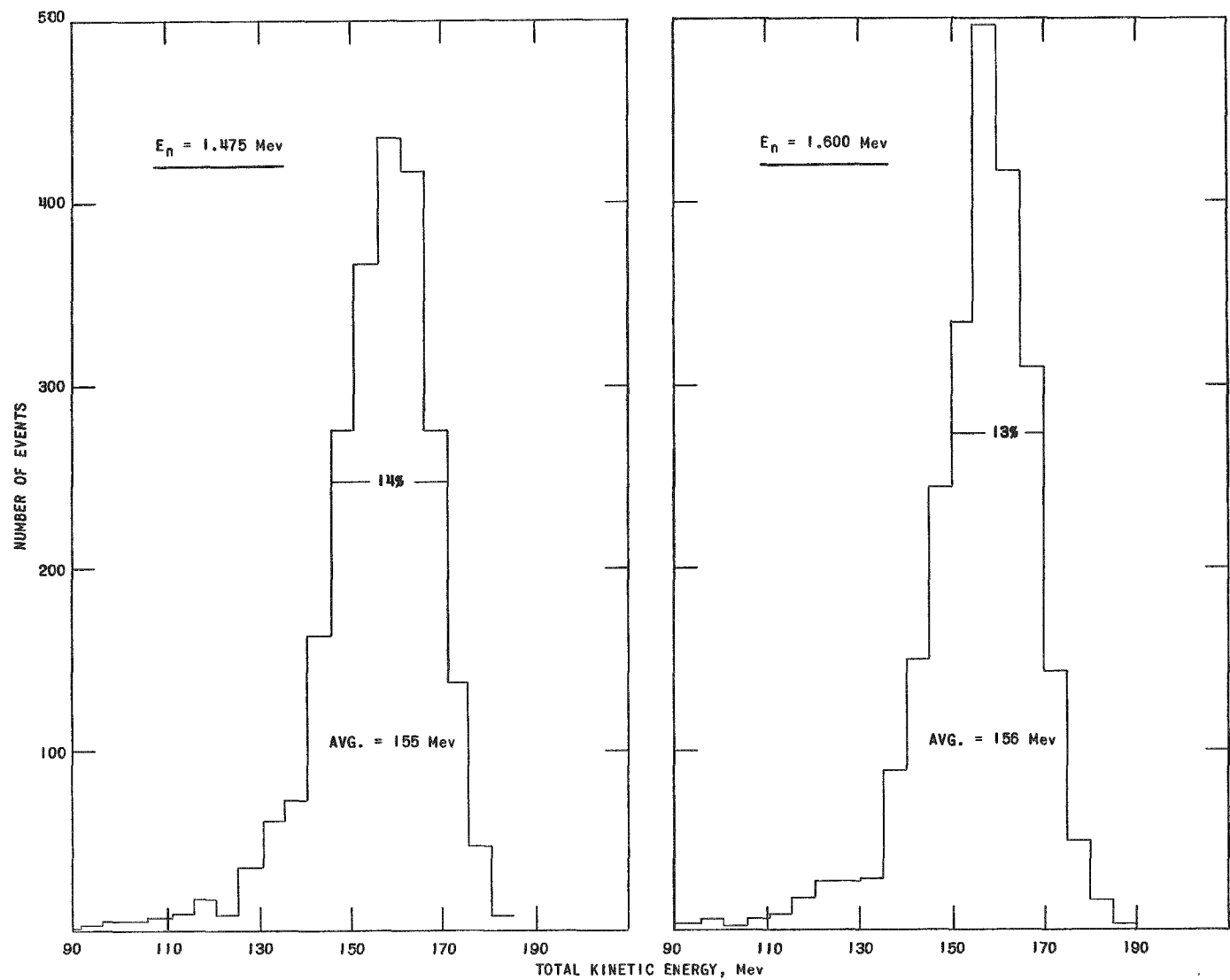


FIG. 4  
 DISTRIBUTION OF TOTAL KINETIC ENERGY OF FRAGMENTS FROM 1.475 Mev  
 AND 1.600 Mev NEUTRON-INDUCED FISSION OF  $\text{Th}^{232}$ .



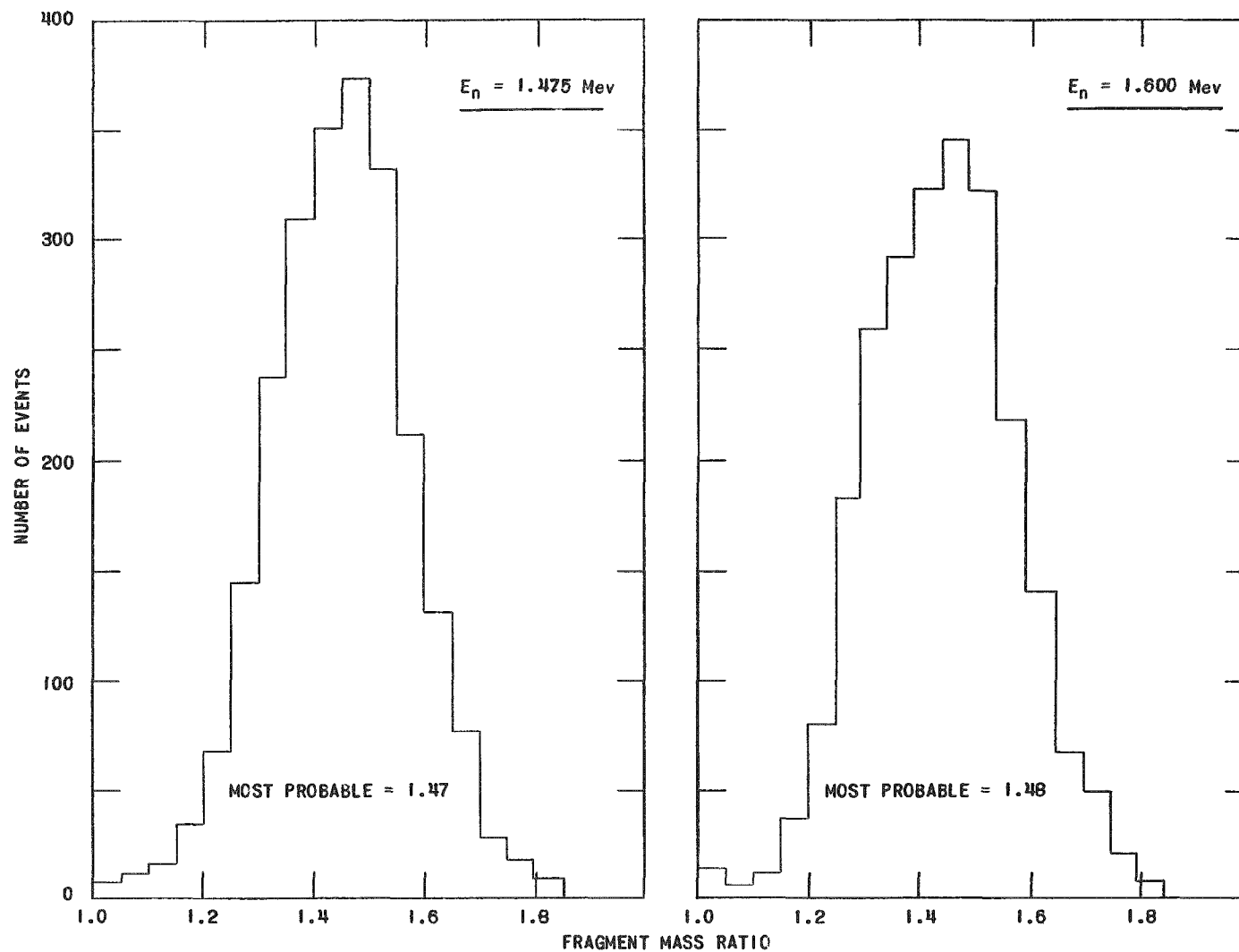


FIG. 5  
 DISTRIBUTION OF FRAGMENT MASS RATIO FOR 1.475 Mev AND  
 1.600 Mev NEUTRON-INDUCED FISSION OF Th<sup>232</sup>.

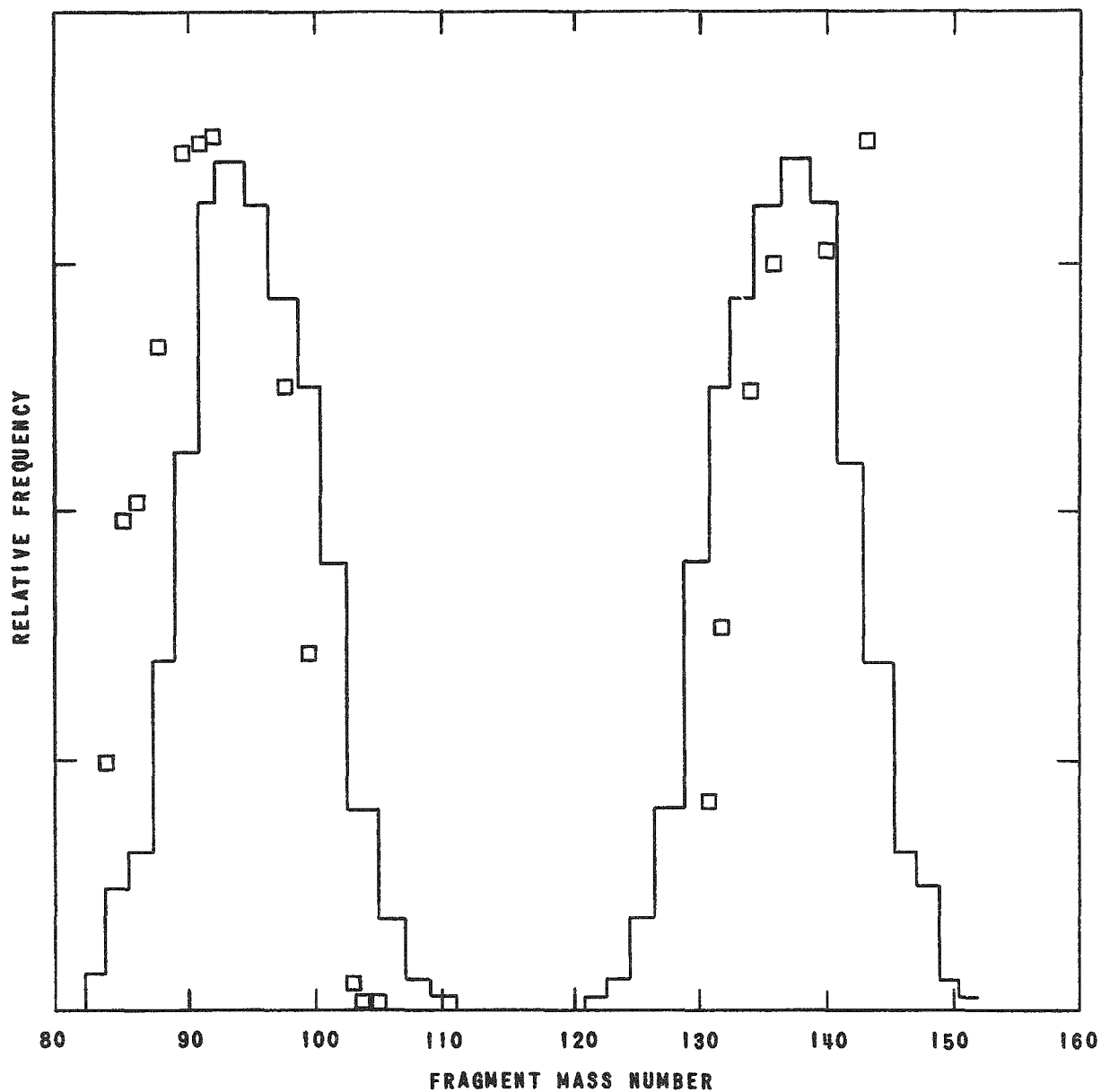


FIG. 6  
PRIMARY MASS YIELD FROM FISSION OF  $\text{Th}^{232}$ .  
CHEMICAL DATA POINTS FROM KATCOFF<sup>19</sup> ARE SHOWN FOR  
COMPARISON.

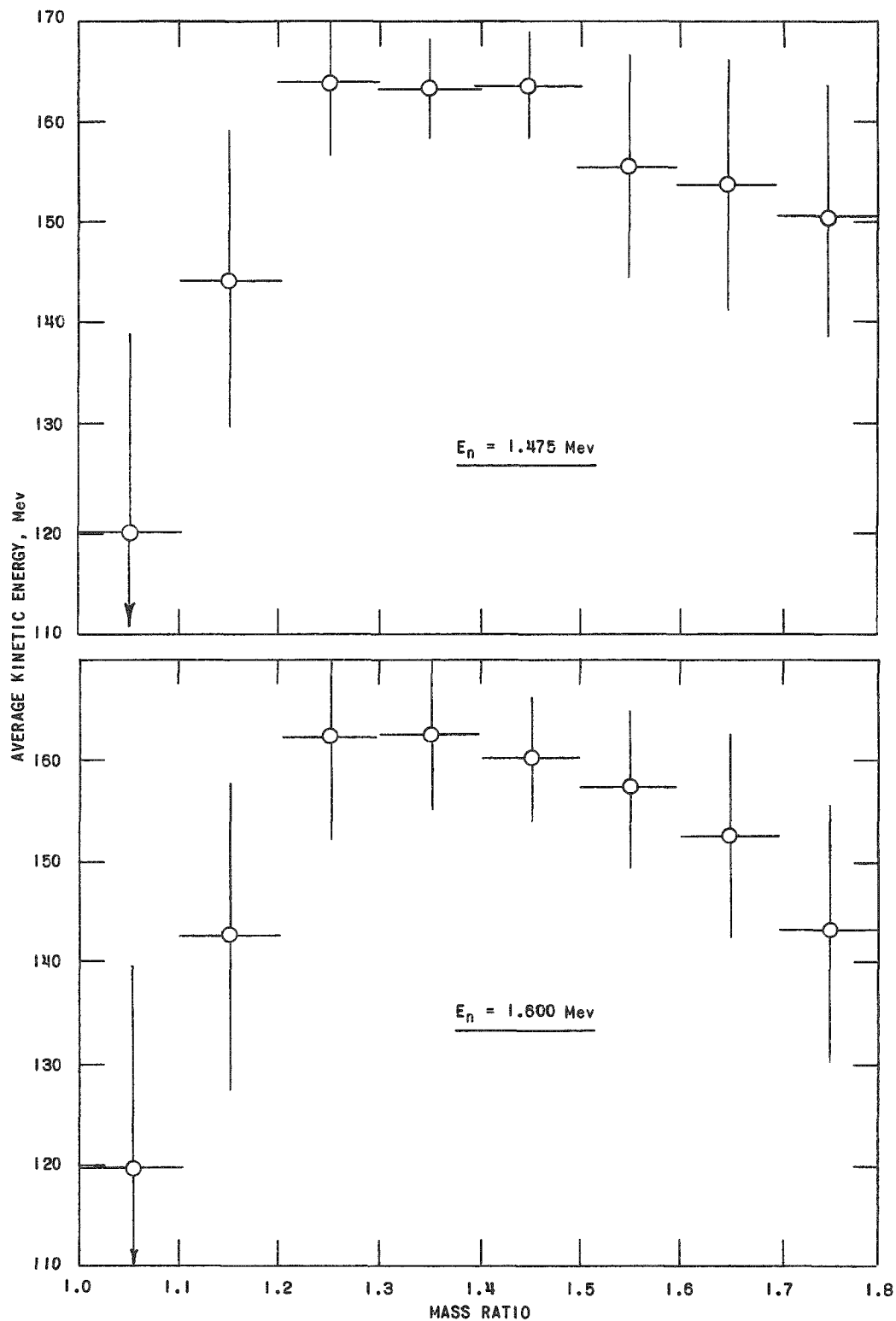


FIG. 7  
 AVERAGE TOTAL KINETIC ENERGY AS A FUNCTION OF  
 MASS RATIO FOR FRAGMENTS FROM 1.475 Mev AND  
 1.600 Mev NEUTRON-INDUCED FISSION OF Th232.

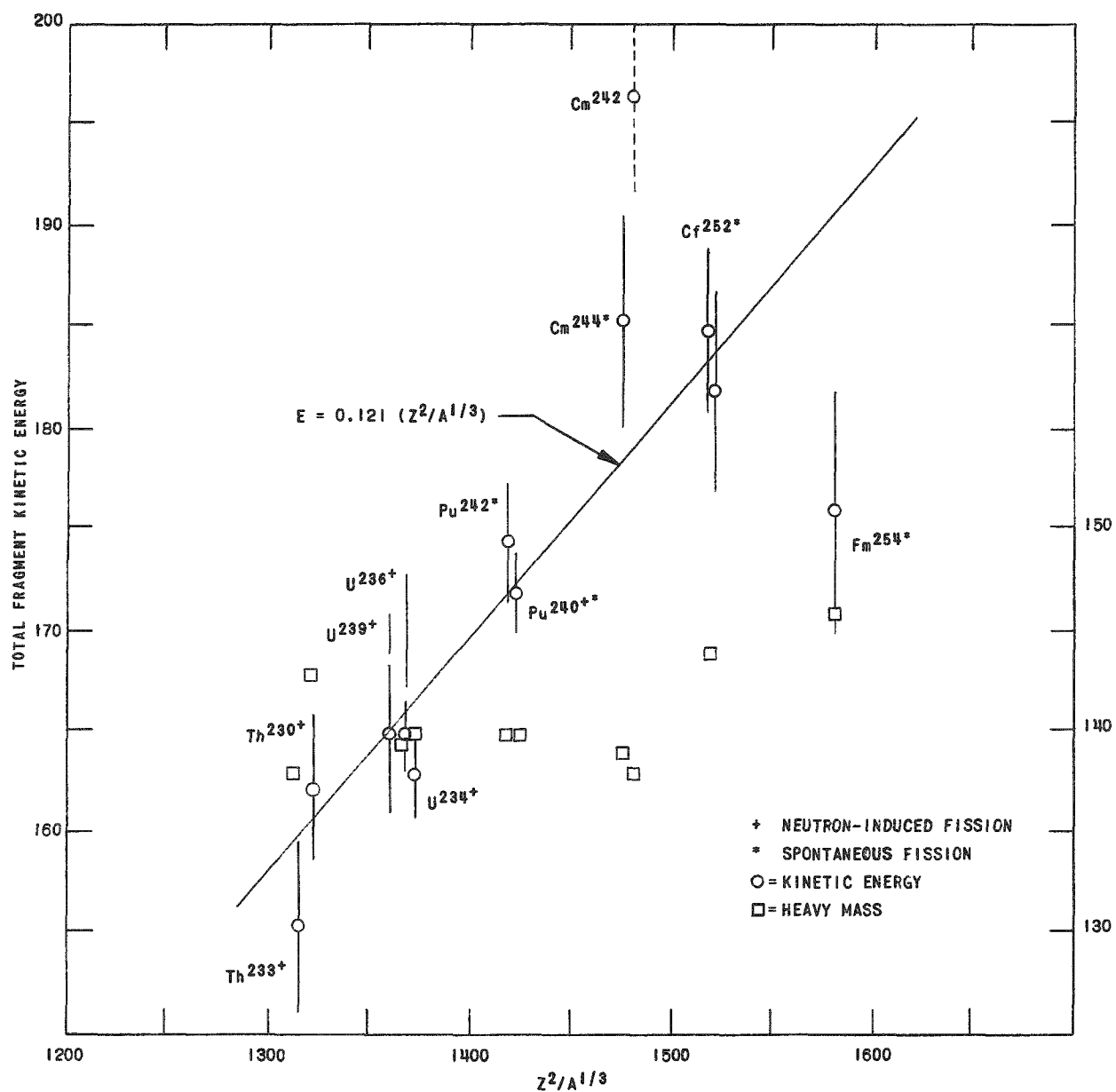


FIG. 8  
 TOTAL FRAGMENT KINETIC ENERGIES AND PRIMARY MASS  
 YIELDS OF KNOWN SPONTANEOUS AND SLOW NEUTRON  
 ( $E_n = \leq 1.5$  Mev) INDUCED FISSION PROCESS.

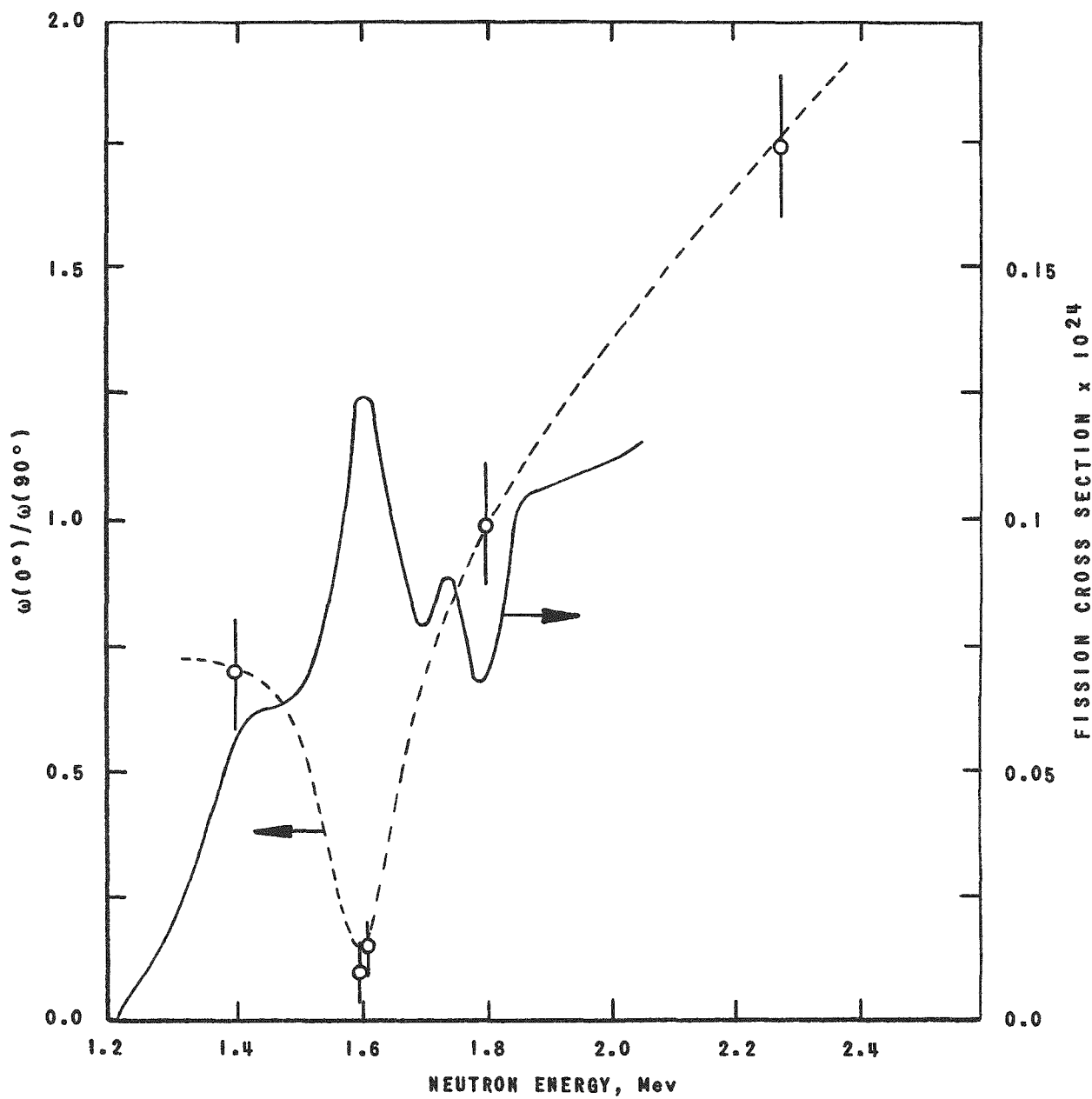


FIG. 9  
ANISOTROPY OF  $\text{Th}^{232}$  FISSION MEASURED  
BY HENKEL AND BROLLEY<sup>10</sup>.

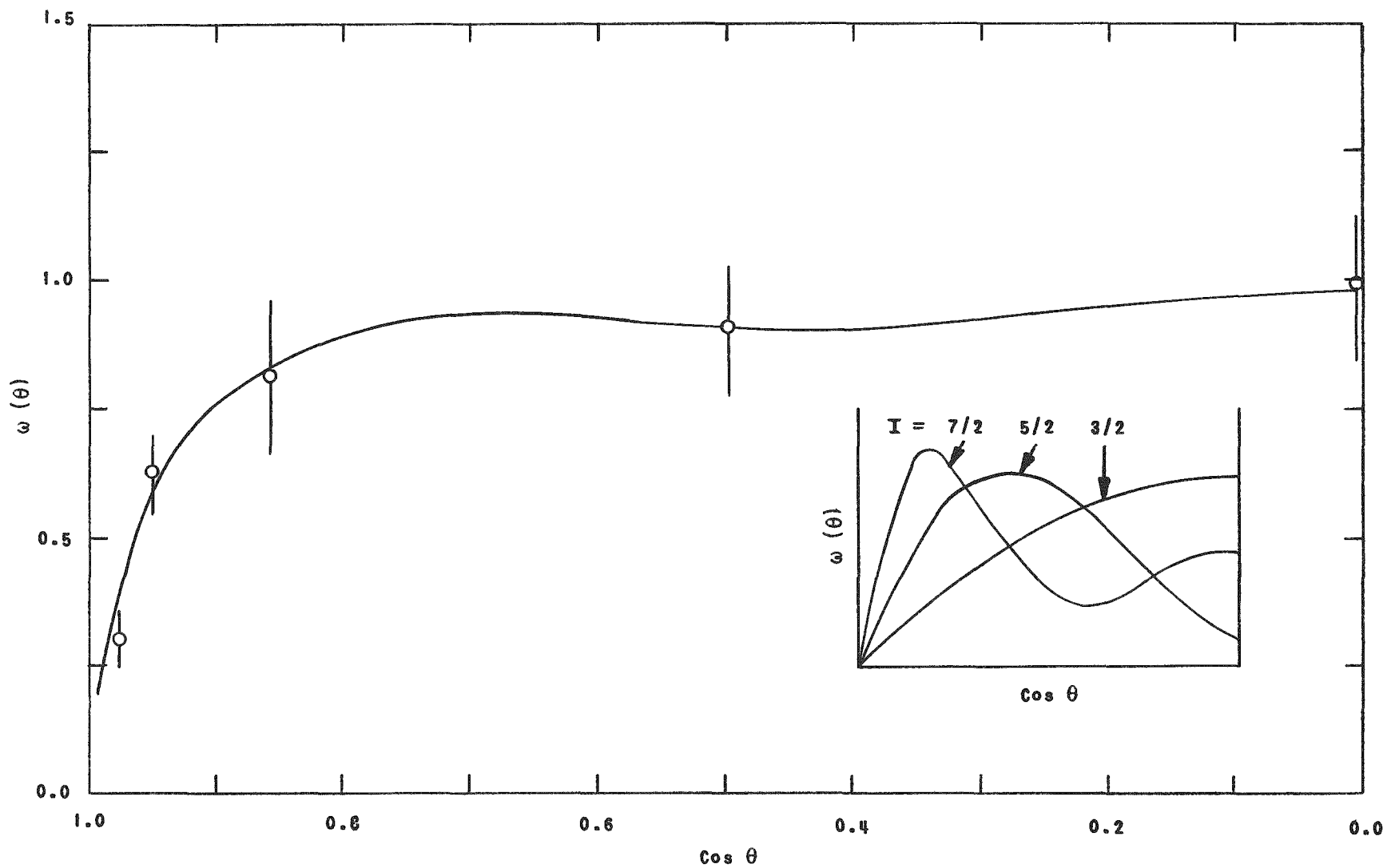


FIG. 10  
 MEASURED ANGULAR DISTRIBUTION OF  $\text{Th}^{232}$  FRAGMENT ANISOTROPY.  
 THEORETICAL COMPONENTS OF THE DISTRIBUTION (INSET) ARE FROM  
 WILLETS AND CHASE<sup>7</sup>